Methane Selective Oxidation on Metal Oxide Catalysts at Low Temperatures with O_2 Using an NO/NO_2 Oxygen Atom Shuttle

I. Tyrone Ghampson[b,c], Sean-Thomas B. Lundin[b], Vibin Vargheese[b], Yasukazu Kobayashi[d], Gregory S. Huff[e], Robert Schlögl[e,f], Annette Trunschke[e], S. Ted Oyama[a,b,g*]

[a]School of Chemical Engineering, Fuzhou University, Fuzhou 350116, China

[b]Department of Applied Chemistry for Environment, Graduate School of Urban Environmental Sciences, Tokyo Metropolitan University, 1-1 Minami-Osawa, Hachioji, Tokyo 192-0397, Japan

[c]Department of Chemical Systems Engineering, The University of Tokyo, 7-3-1 Hongo, Bunkyo-ku, Tokyo 113-8656, Japan

[d]Interdisciplinary Research Center for Catalytic Chemistry, National Institute of Advanced Industrial Science and Technology (AIST), Central 5, 1-1-1 Higashi, Tsukuba, Ibaraki 305-8565, Japan

[e]Fritz-Haber-Institut der Max-Planck-Gesellschaft, Faradayweg 4-6, 14195 Berlin, Germany

[f]Department of Heterogeneous Reactions, Max-Planck-Institut für Chemische Energiekonversion, Stiftstraße 34-36, 45470 Mülheim a. d. Ruhr, Germany

[g]Department of Chemical Engineering, Virginia Tech, Blacksburg, VA 24061, United States

* Corresponding author.

E-mail address: oyama@vt.edu (S. Ted Oyama).

Catalyst synthesis and characterization

Table S1 gives the amounts and sources of the metal precursors used in the catalyst preparation. Fig. S1 shows the X-ray diffraction patterns of the synthesized catalysts after calcination. The lack of oxide peaks indicate that the supported oxides are well dispersed.

Table S1. Quantities of materials used in sample preparation.

Catalyst	SiO_2 / g	Metal source	Amount / mmol
VO_x/SiO_2	10	NH_4VO_3[a]	1.1
CrO_x/SiO_2	10	$Cr(NO_3)_3{\cdot}9H_2O$	1.1
MnO_x/SiO_2	10	$Mn(NO_3)_2{\cdot}6H_2O$	1.1
NbO_x/SiO_2	10	$Nb(HC_2O_4)_5{\cdot}xH_2O$	1.1
MoO_x/SiO_2	10	$(NH_4)_6Mo_7O_{24}{\cdot}4H_2O$	0.15
WO_x/SiO_2	10	$(NH_4)_6W_{12}O_3{\cdot}9H_2O$	0.088

[a]Oxalic acid ($C_2H_2O_4{\cdot}2H_2O$, 2.11 mmol) was added to prepare the precursor solution

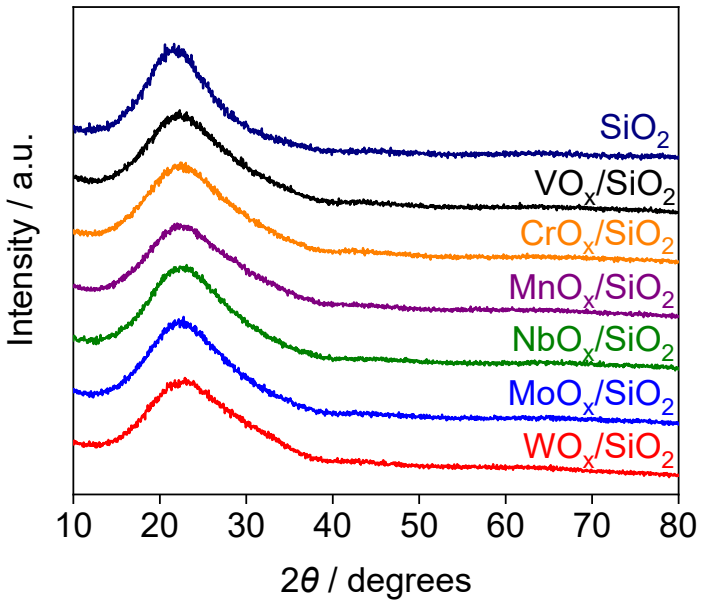

Fig. S1. X-ray diffraction patterns of supported metal oxides.

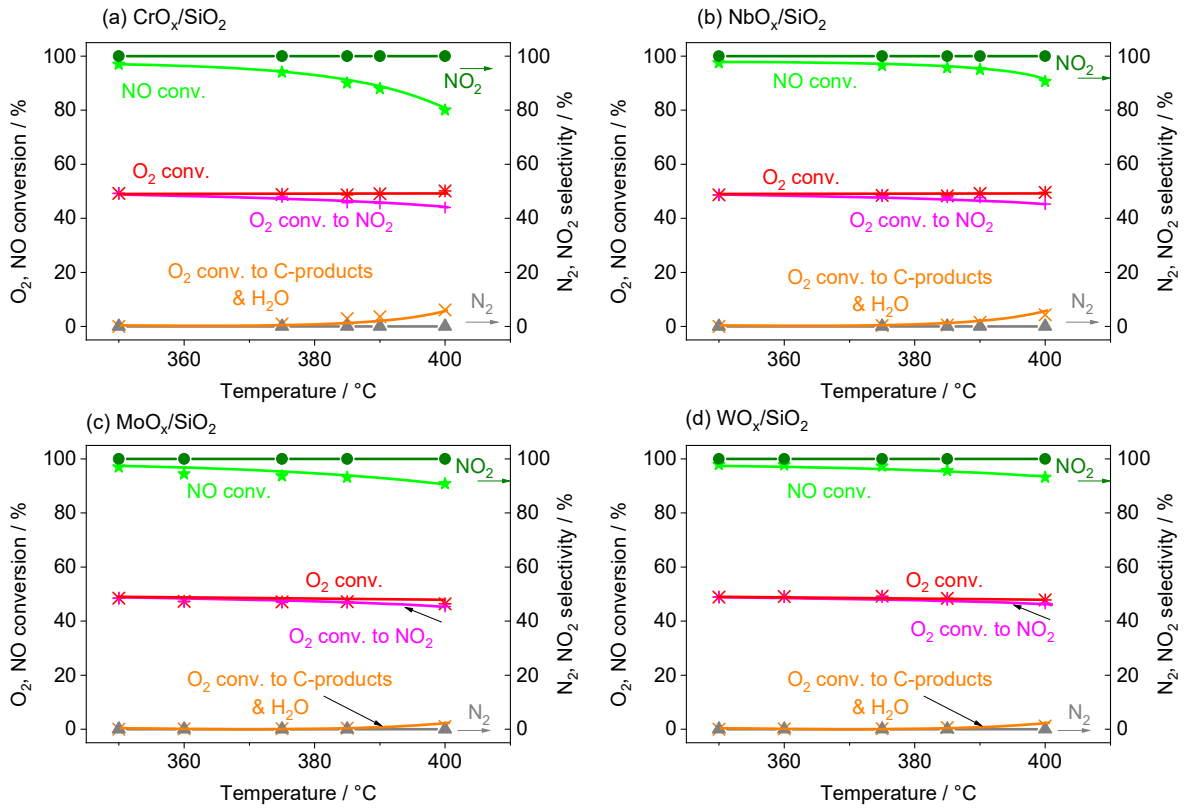

Fig. S2. Oxygen and NO conversion during methane oxidation using NO+O_2 mixture as the oxidant on (a) CrO_x/SiO_2, (b) NbO_x/SiO_2, (c) MoO_x/SiO_2, and (d) WO_x/SiO_2. Conditions: 0.5 g of catalyst, CH_4:NO:O_2:inert = 20:1:1:78, 0.1 MPa, 6000 L kg^{-1} h^{-1} space velocity.

Fig. S1 shows the conversion of the oxygen-containing species O_2 and NO during CH_4 oxidation as a function of temperature for various oxides. The trends are similar. The NO conversion is close to 100% while the O_2 conversion is close to 50% as expected for almost quantitative reaction of the NO and the 1:1 ratio of NO to O_2. A small amount of O_2 is utilized for the conversion of CH_4. There is no N_2 formation, indicating that the source of oxygen in methane oxidation is ultimately O_2.

Table S2. Summary of catalytic methane partial oxidation at low temperatures (≤ 400 °C)

[a] SV = Space velocity L $kgcat^{-1}h^{-1}$,[b] X= Conversion, [c] S_o = Oxygenate selectivity, [d] TOF = Turnover frequency

Turnover frequency was calculated by:

$$\mathrm{TOF}\left(\mathrm{mol/mol}_{surf}\ \mathrm{s}\right) = \frac{\mathrm{Productivity}\ (\mu\mathrm{mol/g_{cat}\ s})}{\mathrm{Surface\ site\ concentration}\ (\mu\mathrm{mol/g_{cat}})} \qquad (1)$$

Catalyst	T ^{o}C	P atm	CH_4:Oxidant: H_2O:inert	SV [a] / h^{-1} $Lkg^{-1}h^{-1}$	X_{CH_4} [b] %	S_o [c] %	Productivity μmol $g_{cat}^{-1}h^{-1}$	TOF[d] mol $mol^{-1}s^{-1}$	Ref
Fe-ZSM-5	300	1	1:0.1(N_2O):0:3.9	3600	0.2	14 (MeOH) 4.6 (DME)	19 (MeOH) 7 (DME)	1.5×10^{-5} (MeOH) 5.4×10^{-6} (DME)	1
Fe-ZSM-5	300	1	1:0.1(N_2O):0:3.9	5000	3.6	1.9 (MeOH)	19 (MeOH)	5.6×10^{-5} (MeOH)	2
H-Cu-SSZ-13	300	1	1:1(N_2O):0.1:1.2	24000	0.75	2.3 (MeOH) 0.1 (HCHO)	55 (MeOH) 1.1 (HCHO)	3.1×10^{-5} (MeOH) 6.1×10^{-7} (HCHO)	3
$FePO_4$	400	1	1:1(N_2O):0:1	7200	0.87	35 (MeOH) 23 (HCHO) 34 (DME)	300 (MeOH) 200 (HCHO) 300 (DME)	1.7×10^{-3} (MeOH) 1.1×10^{-3} (HCHO) 1.7×10^{-3} (DME)	4
$FePO_4$	400	1	1:1:0:0	3600	10.7	15.7 (MeOH)	2200 (MeOH)	5.3×10^{-3} (MeOH)	5
FeO_4	400	1	1:1(N_2O):0:0	3600	6.9	41.5 (MeOH)	3800 (MeOH)	1.2×10^{-2} (MeOH)	5
$FePO_4$/MCM-41	400	1	1:1(N_2O):0:1	18000	0.98	24 (MeOH) 48 (HCHO) 25 (DME)	570 (MeOH) 1200 (HCHO) 600 (DME)	3.1×10^{-5} (MeOH) 2.4×10^{-5} (HCHO) 3.2×10^{-5} (DME)	4
Fe /Ferrierite	280	1	1:0.4(N_2O):0:0.07	12000	0.93	20 (MeOH) 28 (DME)	610 (MeOH) 870 (DME)	2.9×10^{-5} (MeOH) 4.1×10^{-5} (DME)	6
FeCu/ZSM-5	50	20	1:0.025(H_2O_2/H_2 O)	410	0.5	92 (MeOH)	76 (MeOH)	3.9×10^{-6} (MeOH)	7
Li/MgO	377	1	1:0.5(O_2):0.009(O_3):8.4	360000	4.0	90 (HCHO)	60000 (HCHO)	0.3	8
Pt/Y_2O_3	350	1	1:0.05(O_2):0.05(NO):3.9	6000	0.54	11 (DME)	110 (DME)	1.1×10^{-4} (DME)	9
VO_x/SiO_2	400	1	1:0.15:0.05:3.9	6000	0.28	33 (HCHO)	91 (HCHO)	3.8×10^{-4} (HCHO)	This work
MoO_x/SiO_2	400	1	1:0.15:0.05:3.9	6000	0.10	86 (HCHO)	38 (HCHO)	1.1×10^{-4} (HCHO)	This work
WO_x/SiO_2	400	1	1:0.15:0.05:3.9	6000	0.10	72 (HCHO)	31 (HCHO)	9.5×10^{-5} (HCHO)	This work

Rescaled figure showing infrared results for NO + O_2 adsorption and reaction with CH_4.

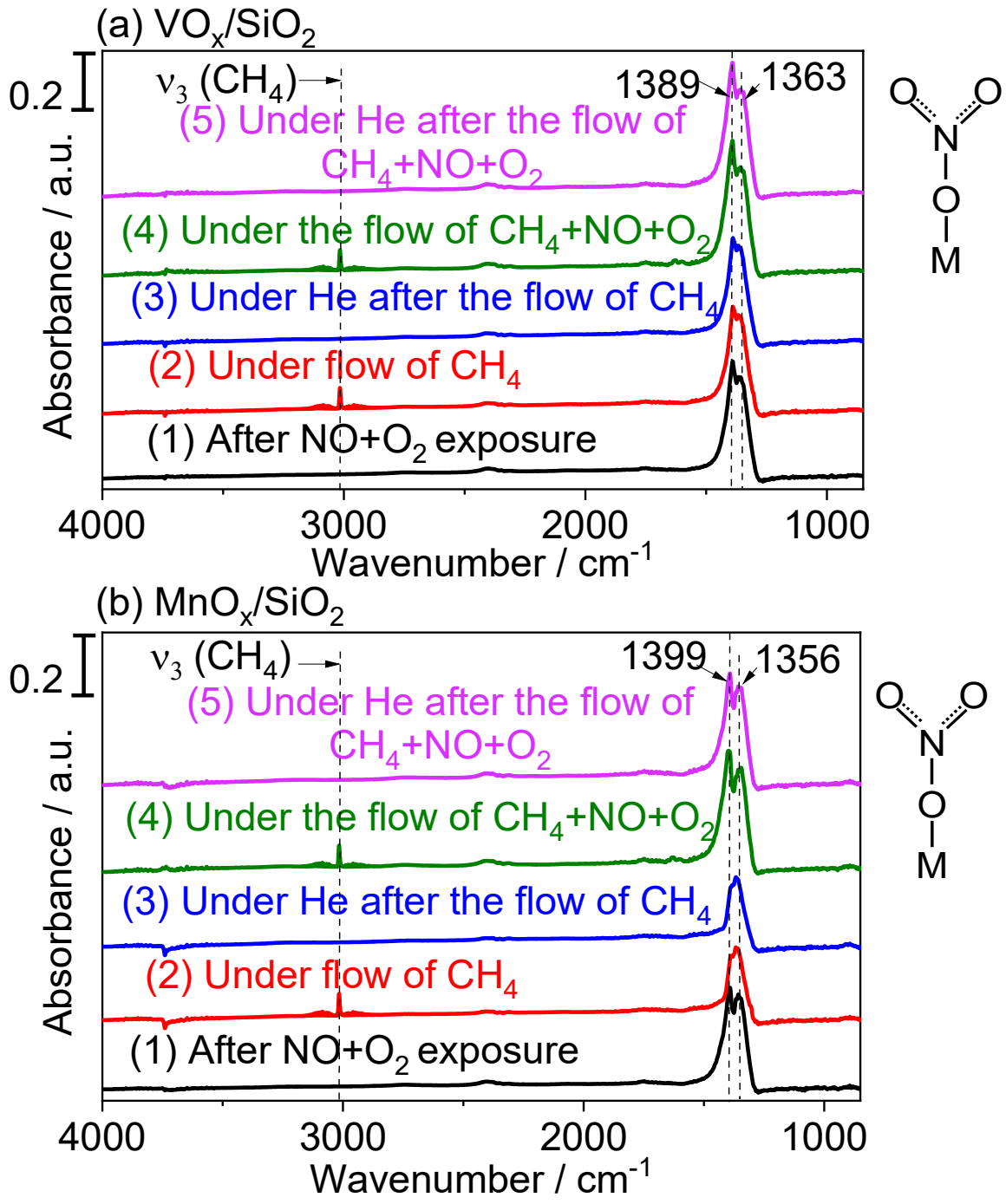

Fig. S3. In situ FTIR spectroscopy results for the reaction of adsorbed NO_x species on (a) VO_x/SiO_2 and (b) MnO_x/SiO_2 with CH_4 at 400 °C at an extended scale. Conditions: (1) under He after flow of $NO:O_2:He$ = 1:1:98 (68 μmol s^{-1}), (2) under flow of 10% CH_4 in He (34 μmol s^{-1}) for 30 min, (3) under He after flow of CH_4, (4) under flow of $CH_4:NO:O_2:He$ = 10:1:1:88 (68 μmol s^{-1}) for 30 min, and (5) under He after the CH_4+NO+O_2+He reaction.

Figure showing deconvolution of the doublet bands due to adsorbed NO_2.

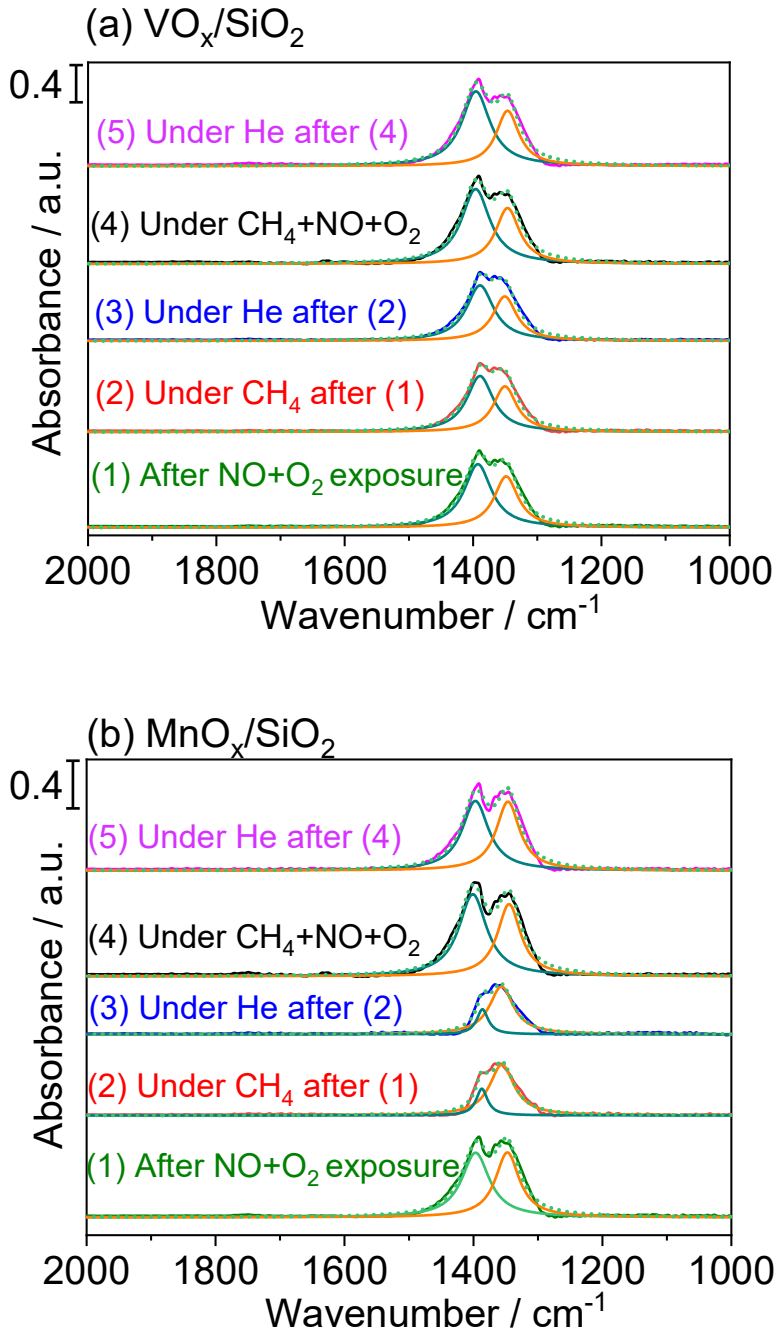

Fig. S4 Deconvolution of the doublet for the monodentate nitrate for the conditions of Fig. S2. The peaks were fitted between 1200 and 1600 cm^{-1}.

Table S3. Areas of deconvoluted spectra

Spectra No.	VO_X/SiO_2 (Area)		MnO_x/SiO_2 (Area)	
	1389 cm^{-1}	1363 cm^{-1}	1399 cm^{-1}	1356 cm^{-1}
5	57.6± 1.1	40.4 ± 1.0	45.8 ± 0.9	40.1 ± 0.8
4	67.9 ±1.1	42.7 ± 1.0	56.8 ± 0.9	41.7 ± 0.8
3	48.4 ± 1.2	33.7 ± 1.1	7.1 ± 0.5	28.6 ± 1.1
2	47.5 ± 1.2	34.1 ± 1.1	7.5 ± 0.5	31.0 ± 0.7
1	55.2 ± 1.1	39.3 ± 1.0	44.4 ± 1.0	38.4 ± 0.9

The deconvoluted spectra show that for the MnO_2/SiO_2 catalyst for the 1399 cm^{-1} high wavenumber peak there is a substantial decrease in the integrated area in going from NO_x in He (Area = 44.4) to NO_x in CH_4 (Area = 7.5), indicating that the NO_2 is reacting with CH_4. The decrease in area for the peak is 83% while that for the 1356 cm^{-1} low wavenumber peak is 20%. For the VO_x/SiO_2 catalyst the corresponding decreases in area of the high and low wavenumber peaks are 14% and 13%, so there appears to be no preferential use of either NO_2 species in partial oxidation.

The differences are more clearly visualized in Fig. S4, which shows areas of deconvoluted peaks of the monodentate nitrates. The deconvolution results are shown in Fig. S3 and Table S2. The reaction of monodentate nitrate species on the metal oxides with CH_4 is evident from the appreciable decrease of the areas (closed symbols) upon the introduction of CH_4 (order No. 1 vs. order Nos. 1 and 2). The decrease was more pronounced on MnO_x/SiO_2, consistent with the higher reactivity of methane discussed earlier. The areas were restored after reintroduction of the $NO+O_2$ mixture and purging with He (order No. 5), confirming the consumption of the nitrates during the CH_4 exposure. However, there was an increase in the areas of the nitrates during the flow of 10% CH_4, 1% NO and 1% O_2 in He (order No. 4), likely due to contributions from weakly adsorbed species.

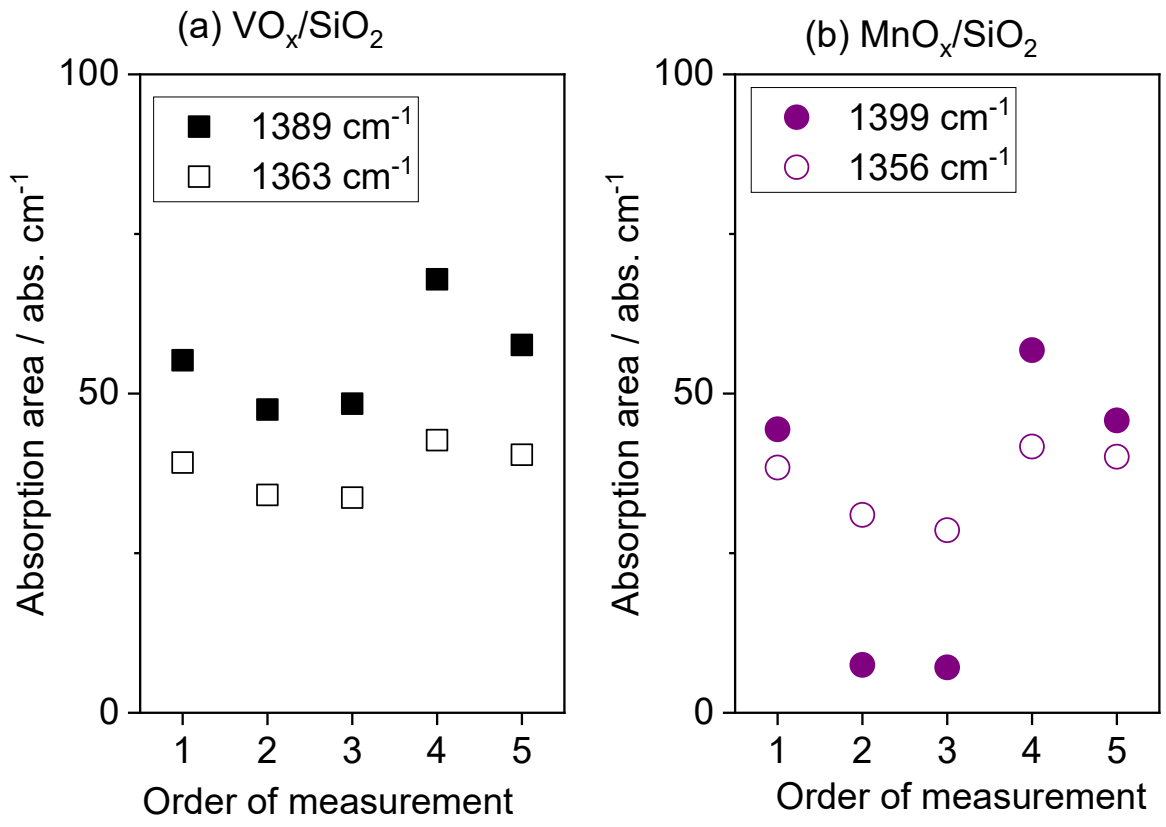

Fig. S5. Deconvoluted areas of monodentate nitrate species at 1389 cm^{-1} and 1363 cm^{-1} on VO_x/SiO_2 (a) and at1399 cm^{-1} and 1356 cm^{-1} on MnO_x/SiO_2 (a) for the conditions of Fig. 10. Order of measurement: (1) under He after flow of $NO:O_2:He$ = 1:1:98 (68 µmol s^{-1}), (2) under flow of 10% CH_4 in He (34 µmol s^{-1}) for 30 min, (3) under He after flow of CH_4, (4) under flow of $CH_4:NO:O_2:He$ = 10:1:1:88 (68 µmol s^{-1}) for 30 min, and (5) under He after the CH_4+NO+O_2+He reaction.

[1] Y.K. Chow, N.F. Dummer, J.H. Carter, C. Williams, G. Shaw, D.J. Willock, S.H. Taylor, S. Yacob, R.J. Meyer, M.M. Bhasin, G.J. Hutchings, Investigating the influence of acid

sites in continuous methane oxidation with N_2O over Fe/MFI zeolites, Catal. Sci. Technol. 8 (2018) 154-163.

[2] M.V. Parfenov, E.V. Starokon, L.V. Pirutko, G.I. Panov, Quasicatalytic and catalytic oxidation of methane to methanol by nitrous oxide over FeZSM-5 zeolite, J. Catal. 318 (2014) 14-21.

[3] B. Ipek, R.F. Lobo, Catalytic conversion of methane to methanol on Cu-SSZ-13 using N_2O as oxidant, Chem. Commun. 52 (2016) 13401-13404.

[4] X. Wang, Y. Wang, Q. Tang, Q. Guo, Q. Zhang, H. Wan, MCM-41-supported iron phosphate catalyst for partial oxidation of methane to oxygenates with oxygen and nitrous oxide, J. Catal. 217 (2003) 457-467.

[5] V.D.B.C. Dasireddy, D. Hanzel, K. Bharuth-Ram, B. Likozar, The effect of oxidant species on direct, non-syngas conversion of methane to methanol over an $FePO_4$ catalyst material, RSC Adv. 9 (2019) 30989-31003.

[6] K.S. Park, J.H. Kim, S.H. Park, D.J. Moon, H.-S. Roh, C.-H. Chung, S.H. Um, J.-H. Choi, J.W. Bae, Direct activation of CH_4 to oxygenates and unsaturated hydrocarbons using N_2O on Fe-modified zeolites, J. Mol. Catal. A: Chem. 426 (2017) 130-140.

[7] J. Xu, R.D. Armstrong, G. Shaw, N.F. Dummer, S.J. Freakley, S.H. Taylor, G.J. Hutchings, Continuous selective oxidation of methane to methanol over Cu- and Fe-modified ZSM-5 catalysts in a flow reactor, Catal. Today 270 (2016) 93-100.

[8] W. Li, S.T. Oyama, Catalytic methane oxidation at low temperatures using ozone, in: B.K. Warren, S.T. Oyama (Eds.) Heterogeneous Hydrocarbon Oxidation ACS Symp. Series 638, Washington DC, 1996, pp 364-373.

[9] V. Vargheese, Y. Kobayashi, S.T. Oyama, The direct partial oxidation of methane to dimethyl ether over Pt/Y_2O_3 catalysts using an NO/O_2 Shuttle, Angew. Chem. Int. Ed. Engl. 59 (2020) 16644-16650.